5 Trends and Characteristics of Hydroclimatic Extremes on Reference Watersheds in Experimental Forests in the USA

D.M. Amatya[1]*, S. Mukherjee[2], E. Keppeler[3], P. Caldwell[4], S.L. Johnson[5], S. Sebestyen[6], J. Campbell[7], B. Rau[8], K. Elder[9], D. Misra[10] and P. Wohlgemuth[11]

[1]Santee Experimental Forest, Southern Research Station, USDA Forest Service, Cordesville, South Carolina, USA; [2]Oak Ridge Institute of Science and Education, Santee Experimental Forest, Southern Research Station, USDA Forest Service, Cordesville, South Carolina, USA; [3]Caspar Creek Experimental Watershed, Pacific Southwest Research Station, USDA Forest Service, Fort Bragg, California, USA; [4]Center for Integrated Forest Science, Southern Research Station, USDA Forest Service, Otto, North Carolina, USA; [5]Formerly HJ Andrews Experimental Forest, Pacific Northwest Research Station, USDA Forest Service, Corvallis, Oregon USA; [6]Marcell Experimental Forest, Northern Research Station, USDA Forest Service, Grand Rapids, Minnesota, USA; [7]Hubbard Brook Experimental Forest, Northern Research Station, USDA Forest Service, Durham, New Hampshire, USA; [8]Fernow Experimental Forest, Northern Research Station, USDA Forest Service, Parsons, West Virginia, USA; [9]Fraser Experimental Forest, Rocky Mountain Research Station, USDA Forest Service, Ft. Collins, Colorado, USA; [10]University of Alaska Fairbanks, Caribou-Poker Creek Research Watershed, Fairbanks, Alaska, USA; [11]Formerly with San Dimas Experimental Forest, Pacific Southwest Research Station, USDA Forest Service, Riverside, California, USA

Abstract

This chapter provides an overview and comparisons of the precipitation intensity–duration–frequency (PIDF) and flood (FFRQ) and low-flow (LFRQ) frequencies for return intervals of 25 years or more at ten relatively undisturbed reference watersheds in the US Forest Service Experimental Forest (EF) network. We demonstrate potential effects of recent climate change on the PIDFs, FFRQ and LFRQ developed with high-resolution temporal data at these ten sites with widely contrasting hydrogeological, topographical, climatic and ecological characteristics. Similarly, we evaluate the on-site-based FFRQ and LFRQ with those published by the US Geological Survey for the regions including our EF sites. This evaluation enables us to better predict PIDFs and FFRQs, frequently used by forest managers/engineers but relatively less studied in forest hydrology, and to prepare for future forest and water management in response to further environmental change.

*Corresponding author: devendra.m.amatya@usda.gov

 Forest Hydrology: Processes, Management and Assessment (eds Leon J. Bren *et al.*)
DOI: 10.1079/9781800625310.0005

5.1 Introduction

There is growing evidence globally that climate change and associated extreme conditions will impact the intensity and frequency of precipitation and hydrological responses (Mukherjee *et al.*, 2023). This response is particularly true in regions with high moisture availability and in wet months causing more frequent and severe flooding (Gimeno *et al.*, 2022). For example, Gu *et al.* (2017) found that alterations in precipitation seasonality based on distributions across 728 stations in China were likely being driven by changes in the pathways of seasonal vapor flux and tropical cyclones.

There is an undisputed relationship between precipitation and flooding, with flooding events following extreme precipitation being reported all over the world (Papalexiou and Montanari, 2019). For example, Jalowska *et al.* (2021) documented an increasing trend in the frequency and intensity of extreme precipitation events and associated flooding within the south-eastern USA using historical climate records. Studies also describe dramatic ecosystem responses to extreme precipitation events with plausible regime shifts in the intensity and quantity of runoff within some ecosystems (Jayakaran *et al.*, 2014; Amatya *et al.*, 2016a; Jalowska *et al.*, 2021; Campbell *et al.*, 2022; Sun *et al.*, 2023). Similarly, streamflow response to increasing precipitation was shown to be altered by forest management (Kelly *et al.*, 2016). Extreme precipitation and floods have attracted a great deal of scientific interest globally due to the particular threat to human activities (Gimeno *et al.*, 2022).

Although trends in precipitation extremes have not yet translated into observable increases in flood risks, except for cyclones as noted by Jalowska *et al.* (2021), a recent study by Wright *et al.* (2019) nevertheless highlights the need for prompt updating of hydrological design standards, taking into consideration recent changes in extreme precipitation properties. Increased extreme rainfall alone does not necessarily lead to increased flooding (Blöschl *et al.*, 2019). There are many factors that affect flood response in addition to precipitation intensity (PI), including the duration and extent of precipitation events, antecedent soil moisture conditions, catchment size, vegetation cover, catchment imperviousness and roughness (Sharma *et al.*, 2018; Yochum *et al.*, 2019) and channel morphology (Wondzell and Swanson, 1999). The drivers of streamflow timing (e.g. response time of streamflow) depend on the magnitude of the event. Lesser extreme flood event timings tend to correspond with antecedent soil moisture, while more extreme flood timings depend more on rainfall timing (Wasko *et al.*, 2020).

Precipitation intensity–duration–frequency (PIDF) analysis based on long-term historical data is frequently used to describe the extreme PI, temporal distribution and frequency of such intensities for decision making by water managers (Srivastava *et al.*, 2019; Amatya *et al.*, 2021; Nerantzaki and Papalexiou, 2022; Mukherjee *et al.*, 2023, 2024), and to estimate design flood magnitudes in ungauged watersheds (Eisenbies *et al.*, 2007). Mukherjee *et al.* (2023) noted that the need for updated PIDF estimations using the most recent data has grown significantly due to recent increases in intense precipitation and the associated impacts on transportation and infrastructure.

The assumption of stationarity has long served as the basis for the statistical analysis of hazards and the design of engineering structures, by defining the magnitude of events with a given frequency of occurrence, such as the stationary 100-year design flood (Salas *et al.*, 2018). However, with climate change, the validity of stationarity in water-resource planning is being questioned (Milly *et al.*, 2008); thus, it is critical to evaluate the stationarity of climate variables, especially precipitation (Wang and Sun, 2020). Using long-term high-resolution historical data, Amatya *et al.* (2021) tested for stationarity in annual maximum PIs at multiple rain gauges within three US Department of Agriculture (USDA) Forest Service experimental forest (USFS-EF) sites (Fig. 5.1), finding increasing trends in peak rainfall intensities at the Santee (SAN) and Coweeta (CHL) sites, but not Alum Creek in Arkansas (not shown), comparable to previous findings of increased frequency of intense precipitation, especially for fall months (Laseter *et al.*, 2012; Burt *et al.*, 2018). Accordingly, Amatya *et al.* (2021) used the assumption of stationarity in their estimates of the PIDF, consistent with de Luca and Galasso (2018), who argued that it is not essential to adopt non-stationary models. The results of de

Fig. 5.1. USDA Forest Service experimental forests evaluated in this and previous studies.

Luca and Galasso (2018) emphasized the importance of the observations of the past for improving the knowledge of hydrological processes under future climate change. Mukherjee *et al.* (2023) tested for non-stationarity of extreme PIs of multiple durations at three additional USFS-EFs (Hubbard Brook, Fraser and HJ Andrews (HJA)) and the three sites used by Amatya *et al.* (2021), but using data extended through 2021.

National Oceanic and Atmospheric Administration (NOAA)'s Atlas 14-based gridded PIDF values based on regional frequency analysis of precipitation recorded at various locations (Bonnin *et al.*, 2006; Perica *et al.*, 2013) are commonly used for design applications to determine the PIDF and associated confidence limits. However, for some durations and frequencies, significant differences between the NOAA and on-site-derived PIs were reported at USFS-EF gauge sites resulting in recommendations for use of the NOAA PIDF values for 1 hour duration and the on-site-derived values for longer durations (Amatya *et al.*, 2021) for conservative design applications. Mukherjee *et al.* (2023) applied this comparative approach to further improve PIDF estimates used for culvert sizing and other engineering and ecological applications in six small, ungauged forested watersheds. The results showed considerable differences between the on-site and NOAA Atlas 14 PIDFs at these six EFs relating to storm durations and gauge elevations, particularly at the steeper HJA and CHL sites. Expanding further on these results, Mukherjee *et al.* (2023) evaluated normalized peak design discharges (Q_p) for 1387 hydrological unit code 16–20 watersheds in the White Mountain National Forest (New Hampshire) and in the six EFs. Consistent with earlier findings by Amatya *et al.* (2021), the authors concluded that the rational method outperformed the US Geological Survey (USGS) regional regression equations (USGS, 1982)

in predicting Q_p in three small, high-relief forest headwater watersheds (both gauged and ungauged), and the USGS regional regression equations performed better than the rational method for larger watersheds. These results have important implications for road crossings and culvert design and maintenance, particularly in high-gradient, high-sediment transport systems characteristic of steep forested landscapes, where enhanced resiliency to extreme precipitation and flood risk induced by spatial heterogeneity (Preece *et al.*, 2021) and climate change is needed. Development of more accurate duration–frequency analyses for EF headwater watersheds is crucial for informed management of roads – approximately 600,000 km with at least 40,000 stream crossings – in our national forests (Heredia *et al.*, 2016).

This chapter provides an overview and comparisons of the PIDF and flood (FFRQ) and low-flow (LFRQ) frequencies for 25-, 50- and 100-year return intervals at ten relatively undisturbed reference watersheds in the USFS-EF network (Fig. 5.1, Table 5.1). We demonstrate potential effects of recent climate change on the PIDFs, FFRQ and LFRQ in these ten reference watersheds with widely contrasting hydrogeological, topographical, climatic and ecological characteristics. Similarly, we evaluate the on-site-based FFRQ and LFRQ with those published by the USGS for the regions including our EF sites. This evaluation will enable us to better predict PIDFs and FFRQs and prepare for future management in response to further environmental change (Wright *et al.*, 2019; Amatya *et al.*, 2021; Mukherjee *et al.*, 2023).

While Amatya *et al.* (2016b) evaluated the response of streamflow to variation in annual precipitation magnitude, form and seasonality, and evapotranspiration at multiple EFs, this cross-site comparison study used high-resolution data from headwater forested catchments for statistical analysis and risk assessment of climate and land-use change on ecosystem functions.

5.2 Site Description

Full descriptions of the ten reference watersheds have been given previously in the first edition of this book (Amatya *et al.*, 2016b). The key characteristics and acronyms are shown in Table 5.1.

5.3 Data and Methods

Data record periods, gauge IDs, and the temporal scales of precipitation and streamflow measurements are presented in Table 5.1.

First, trends in annual maximum PI and streamflow were assessed for significance ($\alpha = 0.05$) using Sen's slope estimator (Sen, 1968) and the modified Mann–Kendall (M-K) trend test (Mann, 1945; Kendall, 1975). Secondly, extreme value analysis was performed as follows.

5.3.1 PIDF estimation

The generalized extreme value (GEV) distribution (Coles *et al.*, 2001) was used for frequency analysis of extreme PI. The GEV distribution is a flexible statistical framework to effectively model upper tail behavior of extreme events, making it well suited for characterizing the frequency and magnitude of rare rainfall events.

The block maxima method (Coles *et al.*, 2001) was utilized to extract the yearly maximum values of 1 and 24 hour PI estimates. This method is widely used in extreme value analysis to capture characteristics of the upper tail of climate data.

The choice of the GEV distribution over other extreme value modeling approaches is consistent with the methodology adopted in NOAA's Atlas 14 (Perica *et al.*, 2018). By employing the same GEV framework, our results are comparable with the standards of the NOAA.

The GEV is a three-parameter distribution comprising location (μ), scale (σ) and shape (ξ) parameters (Coles *et al.*, 2001). These parameters specify the center of the distribution, the deviation around μ and the tail behavior of the distribution, influencing the frequency and magnitude of extreme events. The theoretical cumulative distribution function of a real-valued

Table 5.1. Comparative characteristics of the ten selected reference watersheds (with their acronyms) from the USFS Long-term Experimental Forests network.

Watershed characteristics	Caribou-Poker (CPCR), Alaska	Caspar Creek (CCEW), California	Coweeta (CHL), North Carolina	Fernow (FERN), West Virginia	Fraser (FRS), Colorado	HJ Andrews (HJA), Oregon	Hubbard Brook (HBR), New Hampshire	Marcell (MARC), Minnesota	San Dimas (SDEF), California	Santee (SAN), South Carolina
Physiographical region as per classification by Fenneman	Yukon–Tanana Northern Plateaus Province, 12	Pacific Mountain System, 23f, Pacific Boarder Province	Appalachian Highlands, 5b, Blue Ridge Province	Appalachian Highlands, 8c, Appalachian Plateau	Rocky Mountain Systems, 15, Southern Rocky Mountain	Pacific Mountain System,22b, Sierra-Cascade Mountain	Appalachian Highlands, 9b, New England Province	12b, Interior Plain, Central Lowland	Pacific Mountain System, 23g, Pacific Boarder Province	Atlantic Plain Coastal Plain
Climatic region as per classification by Köppen (Peel *et al*., 2007)	Dfc, continental subarctic or boreal taiga	Csb, temperate/ mesothermal, Mediterranean	Cfb, marine temperate	Dfb, continental warm summer	Dsc, continental cold winter and cool, short, dry summer	Csb, temperate/ mesothermal dry summer	Dfb, continental warm summer	Dfb, continental warm summer	Csa, Mediterranean hot summer	Cfa, temperate humid subtropical
Watershed #/ year gauging started	CPCRW –C2, 1969	North Fork, 1962	WS18, 1936	WS4, 1951	East St. Louis, 1943	WS2, 1952	WS 3, 1957	S2, 1960	Bell 3, 1938	(WS80) 1968
Latitude/ longitude	65.17°N, 147.50°W	39.36°N, 123.74°W	35.05°N, 83.43°W	39.03°N, 79.67°W	39.89°N, 105.88°W	44.21°N, 122.23°W,	44.0°N, 71.7°W	47.514°N, 93.473°W	34.20°N, 117.78°W	33.17°N, 79.77°W
Elevation (m a.m.s.l.)a	210–826	40–330	726–993	670–866	2907–3719	572–1079	527–732	420–430	755–1080	3.7–10
Average slope (%)	31	49	52	20	16	41	21	3	34	<3
Drainage area (ha)	520	479	12.5	38.7	803	60	42.4	9.7	25	160
Vegetation type/average leaf area index (LAI) (m^2/m^2)	Boreal Forest/ LAI = 4.1	Second-growth coast redwood/ Douglas fir forest/ LAI = 11.7	Mixed deciduous forest/LAI = 6.2	Mixed deciduous hardwoods/ LAI = 4.5	Mixed spruce/ fire and pine/ LAI = 3.44	Conifer primarily Douglas fir and western hemlock/ LAI = 12	Northern hardwood/ LAI = 6.3	Deciduous uplands; black spruce-*Sphagnum* bog/LAI = N/A	Mixed chaparral/ LAI = 2.2	Pine mixed hardwood/ LAI = 2.8
Dominant geology/aquifer	Yukon–Tanana metamorphic complex/ discontinuous permafrost	Marine shales and sandstones, Coastal Belt of the Franciscan Complex	Quartz dioritic gneiss predominant, Coweeta Group	Sedimentary; Hampshire formation sandstone and shales	Gneiss and schist, glacial till	Volcanic tuffs and breccias covered with andesite colluvium	Metasedimentary/ mica schist, calc-silicate granulite, Silurian Rangeley formation	Glacial till overlying deep outwash sands above pre-Cambrian bedrock	Pre-Cambrian metamorphics and Mesozoic granitics	Sedimentary/Santee limestone

Dominant soil type/depth (m)	Olnes Silt Loam – *Typic Cryorthents*; Fairplay Silt Loam – *Fluvaquentic Endoaquolls*; Ester Silt Loam – *Typic Histoturbels*0.2–0.5m	Vandame Series Ultisols (*Typic Haplohumults*) 1–1.5 m	Coweeta–Evard–Saunook complex (fine loamy, mixed, *Mesic* and *Humic Hapludults*); >1.5 m	Loamy-skeletal, mixed mesic *Typic Dystrudepts*1 m	Leighcan Series, loamy-skeletal, *Typic Dystrocyepts* <1.5 m	50% andesite colluvium (unnamed soil series), 20% Limberlost series, loam to green brecciaUp to 1.2 m	Lyman-Tunbridge–Becket series, *Typic Haplorthods*C horizon depth 0–9 m	Warba Series fine loamy, mixed, superactive, frigid haplic Glossudalfs (0.5 m); Loxely peat Dysic, frigid Typic Haplosaprists (≤7 m)	Trigo–Exchequer series loamy, mixed, thermic, shallow, *Typic Xerorthents* 0.1–0.5 m	Wahee Series clayey, mixed, thermic *Aeric Ochraquults* 1.5 m
Long-term mean precipitation (mm)	262	1146	2010[2]	1458	750	2300	1350	780	715	1388
Precipitation period (gauge – timescale) used in this study	1993–2021 (CPEAK – hourly)	1985–2021 (NFC620 – hourly)	1976–2021 (RG41 –hourly)	1951–2022 (S4 – daily)	2004–2021 (HQTRS – hourly)	1979–2018 (PRIMET – hourly)	1977–2021 (RG1 – hourly)	1962–2022 (MEF South – daily)	1977–2015 (Bell 3 – hourly)	1977–2021 (Met25 – hourly)
Long-term mean temperature (°C)	–3.0	10.7	12.9b	9.3	1.0	8.4	5.9	3.4	14.4	18.5
Long-term mean potential evapotrans-piration (PET) (mm)	466c	660c	1013[b,d]	560d	383c	546c	550c	552	753c	1149 (Hargreaves-Samani)c
Dryness index	1.13	0.50	0.50	0.38	0.51	0.24	0.41	0.71	1.05	0.71
Long-term mean streamflow (mm)	80	621	997	640	337	1321	860	171	84	290
Period of streamflow record	1969–present	1962–present	1936–present	1951–present	1943–present	November 1952–present	1957–present	1961–2017	1938–1960; 1964–2001; 2013–present	1969–1981, 1989–1999, 2003-–present

Continued

Table 5.1. Continued

Watershed characteristics	Caribou-Poker (CPCR), Alaska	Caspar Creek (CCEW), California	Coweeta (CHL), North Carolina	Fernow (FERN), West Virginia	Fraser (FRS), Colorado	HJ Andrews (HJA), Oregon	Hubbard Brook (HBR), New Hampshire	Marcell (MARC), Minnesota	San Dimas (SDEF), California	Santee (SAN), South Carolina
Streamflow period (gauge – timescale) used in this study	1969–2021 (C2 – instant)	1985–2017 (NF – instant)	1938–2015 (WS18 – instant)	1980–2015 (WS4 – instant)	1943–2021 (ELOUI – instant)	1952–2018 (WS2 – instant)	1957–2021 (WS3 – instant)	1962–2017 (S2 WS – instant)	1939–2001 (Bell3 –-instant)	1965–2020 (WS80 –instant)
Surface runoff/ flow generation	Saturation excess flow	Infiltration excess overland flow limited to compacted surfaces	Rare surface runoff, direct channel and fast shallow subsurface flow from variable source area	Minimal surface runoff	Rare, only during snowmelt	Minimal surface runoff – high porosity	Minimal surface runoff	Infiltration excess over frozen and saturation excess flow over unfrozen soils	Rare hillslope flow except after fire when infiltration excess flow	Saturation excess flow
Subsurface flow/drainage	Shallow subsurface flow	Transient subsurface stormflow and soil pipe preferential flow	Shallow lateral flow via soils with high conductivity	Lateral subsurface flow to channel	Shallow subsurface (macropores, coarse soils) and groundwater	Shallow subsurface lateral flow	Lateral subsurface flow	Shallow subsurface with some seepage to an underlying groundwater aquifer	Groundwater flow unknown but presumably high rate of shallow lateral flow	Shallow lateral subsurface flow with negligible deep seepage
Average water table dynamics/ depth (m)	Unknown	1–8 m	>1.5m except near stream	Unknown	Unknown	Unknown	Variable water table depth	~0.3m in the bog; 0.5m in uplands	Unknown; potentially very deep	Shallow, ~1.0m
Riparian areas for hydrology	None	Limited due to steep topography	Limited due to steep topography	Limited due to steep topography	Limited to valleys, fens and bogs	Limited	Limited due to steep topography	33% of area is a peatland	~2%	15%
Major or extreme natural disturbance	1967 Fairbanks Flood	Windstorm (1995); landslide (2006); drought (2020–2021)	Chestnut blight (1920s-1930s), drought, hurricanes, hemlock wooly adelgid (2003–present)	Chestnut blight; hurricanes (windstorms; SuperStorm Sandy (2012)	Pine bark beetle epidemic	None in reference	Hurricane (1938); ice storm (1998)	Peatland wildfire (1864); potential for derecho, tornados and wildfires	Wildfire (Meixner and Wohlgemuth, 2003)	Hurricane Hugo (1989); indirect effects of Hurricane Joaquin (2015)
Other specific hydrological features	3% permafrost underlain	Fog input	–	–	Snowmelt-dominated hydrological regime	–	Discontinuous dense pan C horizon	Drainage from bog dome and uplands; some deep seepage to the aquifer	Extremely high levels of nitrate from chronic air pollution	Compared with pre-Hugo, flow reversal in paired watersheds after Hugo extreme discharge topping the rating curve and site flooding (Joaquin)

Key publication(s) on extreme climatic events or related to extreme events	Bolton *et al*. (2004); Jones and Rinehart (2010); van Cleve *et al*. (2023)	Cafferata and Reid (2013); Richardson *et al*. (2021)	Laseter *et al*. (2012); Burt *et al*. (2018); Mukherjee *et al*. (2023)	Adams *et al*. (1994)	Mukherjee *et al*. (2023)	Rothacher *et al*. (1967); Daly *et al*. (2019); Johnson *et al*. (2021, 2023); Mukherjee *et al*. (2023)	Campbell *et al*. (2011); Mukherjee *et al*. (2023)	Sebestyen *et al*. (2011, 2021); Verry *et al*. (2011)	Dunn *et al*. (1988); Wohlgemuth (2016)	Hook *et al*. (1991); Jayakaran *et al*. (2014); Amatya *et al*. (2016b, 2021); Mukherjee *et al*. (2023)
Forest experimental watershed contact	Jamie Hollingsworth: jhollingsworth@alaska.edu	Joe Wagenbrenner: joseph.wagenbrenner@usda.gov	Peter Caldwell: peter.v.caldwell@usda.gov	Benjamin Rau: benjamin.rau@usda.gov	Kelly Elder: kevin.elder@usda.gov	Sherri Johnson: sherri.johnson@oregonstate.edu	Amey Bailey: amey.bailey@usda.gov	FS-MarcellExpForestSM.FS.MarcellEF@usda.gov	Pete Wohlgemuth: peter.wohlgemuth@usda.gov (retired)	Devendra Amatya: devendra.m.amatya@usda.gov
Experimental forest website	www.lter.uaf.edu/bnz_cpcrw.cfm	www.fs.usda.gov/research/psw/forestsandranges/locations/casparcreek	www.srs.fs.usda.gov/coweeta/	www.nrs.fs.fed.us/ef/locatios/wv/fernow	www.fs.usda.gov/efr/fraser	http://andrewsforest.oregonstate.edu	www.hubbardbrook.org	www.nrs.fs.fed.us/ef/marcell/	www.fs.fed.us/psw/ef/san_dimas	www.fs.usda.gov/research/srs/forestsandranges/locations/santee

N/A, not applicable.
[a]a.m.s.l., above mean sea level.
[b]Water years 1938–2013. Water year taken as starting in May and ending in April.
[c]PET estimated from Thornthwaite (1948) method for all, except for the Santee (SAN) site from the Hargreaves–Samani method (Hargreaves and Samani, 1982).
[d]PET estimated from an evaporation pan (Patric and Goswami, 1968).
[e]PET estimated from Hamon (1963) method with corrections.

random variable, x, following the GEV distribution can be expressed as:

$$F_{GEV}(x|\mu,\sigma,\varepsilon)=\left[-(1+\frac{\varepsilon}{\sigma}(x-\mu)^{-1/\varepsilon}\right],\mu\in R,\sigma>0,\varepsilon\neq 0 \quad (5.1)$$

Parameter estimation for the GEV distribution was carried out using the maximum likelihood estimation (MLE) method with both stationary and non-stationary assumptions for the location and scale parameters (Martins and Stedinger, 2000; Coles *et al.*, 2001). MLE is a widely used statistical technique that is used to find parameter values that maximize the likelihood of the observed data. In the context of the GEV distribution, MLE involves finding the values of XII, σ and XIV that maximize the likelihood function.

To account for potential non-stationarities due to climate change in PIs, we employed a time-varying approach, allowing the location parameter to change over time (Perica *et al.*, 2018), an approach particularly relevant for extreme value analysis where characteristics of extreme events vary with time (Cheng and AghaKouchak, 2014).

Specifically, we adopted a time-varying model for the location parameter:

$$\mu(t)=\mu_0+\mu_1 t \quad (5.2)$$

where, μ_0 is the initial location parameter at time $t = 0$, and μ_1 is the rate of change of the location parameter.

By incorporating time-varying models, we can capture potential changes in the frequency and magnitude of extreme rainfall events over time. The p-quantile of the GEV distribution was then estimated as,

$$q_p=\left[\left(-\frac{1}{\ln(1-p)}\right)^{\varepsilon}-1\right]\times\frac{\sigma}{\varepsilon}+\mu,(\varepsilon\neq 0) \quad (5.3)$$

where $(1 - p)$ is the non-exceedance probability.

The non-stationary assumptions were employed to identify the best GEV model following the Akaike information criteria, Bayesian information criterion and the likelihood ratio test (Ansa *et al.*, 2021; Kim *et al.*, 2017). Non-stationarity was confirmed only if all these criteria were fulfilled. The uncertainties associated with the estimation of PI quantiles were quantified based on the 90% confidence intervals (CI)s using the delta method (Cox, 1990).

5.3.2 High- and low-flow frequency analysis

Availability of long-term streamflow data including for both extreme high- and low-flow periods is crucial for the efficient management of water resources and infrastructure. The USGS requires 30 years of streamflow data to designate long-term stream gauges (Jian *et al.*, 2015). We conducted the high- and low-flow frequency analysis only for the sites that have at least 30 years of annual maximum and annual minimum flows after eliminating the outliers and zero flows. Additionally, our analysis only included the sites at which the number of outliers and zero flows do not exceed 25% of the total number of data years.

Observations that deviate significantly from the overall data trend are potentially influential 'outliers.' In the context of annual peak flows, low outliers may represent floods generated by processes distinct from those of larger floods (National Research Council, 1988, 1995). Due to their atypical nature, the inclusion of these zero flows values (common in dry areas) and outliers can significantly impact the statistical parameters derived from the data, particularly for small samples. The low and high outliers were identified based on the threshold estimation guidelines recommended by the Interagency Advisory Committee on Water Data (1982).

High-flow frequency analysis was conducted on long-term streamflow data sets by fitting annual maxima to the log-Pearson type III (LPIII) distribution, a widely established statistical method for predicting flood frequency. The LPIII distribution is endorsed by US federal agencies and many flood frequency analysts (England *et al.*, 2019), and is used in USGS PEAKFQW version 5.2.0 (Feaster *et al.*, 2009).

A key advantage of this method is effective extrapolation of event data for return periods exceeding the range of observed flood events.

Low-flow statistics quantify the magnitude and frequency of low-flow conditions as the minimum average streamflow over a specified time period. Low-flow frequencies are calculated by fitting an annual minima series of N days average streamflow to a known statistical distribution, where N can range from 1 to 365 days (Feaster and Guimaraes, 2014). The 10 year recurrence interval of the annual minimum 7 day average (7Q10) is commonly used (Feaster and Guimaraes, 2014). In probabilistic terms, the estimated 7Q10 value represents the 10% probability that the annual minimum 7 day average streamflow of any given year will be equal to or lower than this value (Riggs, 1985). We estimated 7Q10 by fitting the logarithms (base 10) of the annual minimum 7 day average streamflow (ANMIN7Q) to the LPIII distribution.

The goodness of LPIII fit was tested using the Anderson–Darling test (Laio, 2004). To fit LPIII distribution, the mean, standard deviation and skew coefficient of the logarithms of the streamflow were calculated. Estimates of the non-exceedance flows for a specified recurrence interval T were calculated using the following equation:

$$\log(Q_T) = X + K \times S \tag{5.4}$$

where Q_T is the annual maximum flow (ANMAXQ) for high-flow analysis or ANMIN7Q for low-flow analysis (l/s), T is the return interval (years), X is the mean of the logarithms of the annual flow values (ANMAXQ or ANMIN7Q), K is a frequency factor that is a function of the return interval and the weighted coefficient of skew, and S is the standard deviation of the logarithms of the annual flow values (ANMAXQ or ANMIN7Q). The weighted skew coefficient and frequency factor were estimated (Haan *et al.*, 1994). The uncertainty associated with the estimation of the non-exceedance flows was quantified through the calculation of the standard error via a resampling approach. This involved generating 10,000 random samples from the LPIII distribution using the estimated model parameters.

5.4 Results and Discussion

5.4.1 Characteristics of precipitation extremes

The mean and variability of annual maximum PIs (ANMAXPI) for all sites are shown in Fig. 5.2 for the 1 and 24 h-duration storms. We focused on the ANMAXPI values for each site because of the high probability of extreme precipitation events translating into floods (Amatya *et al.*, 2021). The rain gauge at SAN and CHL recorded the highest mean 1 hour ANMAXPI magnitude of 4.8 cm/h and 3.4 cm/h, respectively, over a long-term period of more than 40 years. The annual variability of 1 hour ANMAXPI was found to be relatively higher at CHL, CPCR and SAN. The mean 24 hour ANMAXPI magnitude was relatively similar across all the sites investigated, except for the very low mean 24 hour ANMAXPI magnitude of 0.1 cm/h at FRS. The annual variability of 24 hour ANMAXPI was found to be relatively higher in CPCR and SAN. Overall, for both 1 hour and 24 hour storms, the mean ANMAXPI magnitude was found to be similar at SAN and CHL, the two south-eastern sites.

The results of trend analysis for the 1 and 24 hour ANMAXPI are shown in Supplementary Figs S5.1 and S5.2 and Tables 5.2 and 5.3. A long-term decline in 1 hour PI was most pronounced and significant at the CPCR site. Only the CHL site exhibited a pronounced statistically significant increasing long-term trend in 24 hour PI (Fig. S5.2, Table 5.3). These findings highlight the complex temporal dynamics underlying the 1 and 24 hour PI. Further investigation into the specific factors driving these diverse long-term and recent trends is warranted to elucidate the underlying mechanisms and inform future management strategies.

5.4.2 High-flow characteristics

The mean and variability of annual maximum streamflow per unit drainage area (ANMAXQ) for all sites are shown in Fig. 5.3 and Table 5.4.

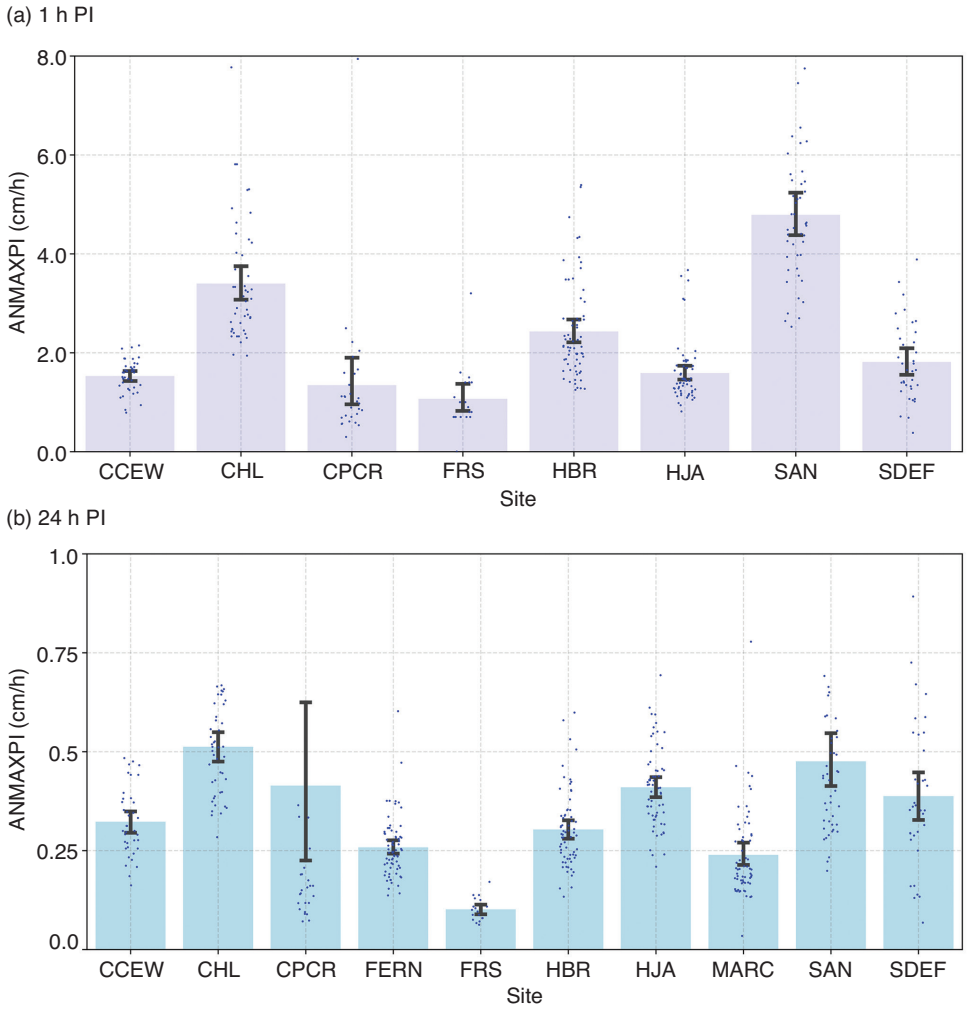

Fig. 5.2. Mean (box plots) and variability (1 SD, shown by whiskers) of annual maximum precipitation intensities (ANMAXPI, cm/h) for all sites for the 1 hour (a) and 24 hour (b) duration storms. PI, precipitation intensity. See Table 5.1 for site abbreviations.

The SAN and HBR EF gauging stations recorded extremely high mean ANMAXQ magnitudes of 11.8 and 15.5 l/s/ha, respectively. The annual variability of ANMAXQ was large for the HBR EF (9 l/s/ha) and even larger for the SAN EF (20 l/s/ha). The CCEW, CHL, FERN and HJA sites showed moderately high mean ANMAXQ values of 7, 5, 5 and 7 l/s/ha, respectively, while the CPCR, FRS, MARC and SDEF sites showed very low values for mean ANMAXQ of about 0.65, 1.1, 2.4 and 3.5 l/s/ha, respectively.

The long-term trend analysis of ANMAXQ revealed a decline across most of the sites, except for the CHL and HBR sites, which exhibited increasing trends (Fig. S5.3). Notably, for the HBR site, ANMAXQ showed a statistically significant ($P<0.05$) upward trajectory. None of the sites showed a statistically significant trend in ANMAXQ for the recent 20 year period, despite a suggested downward trend for most sites and an upward trend for CHL, FRS, HBR, and SAN (Table 5.4).

Table 5.2. Results of trend analysis of annual maximum 1 h precipitation intensity including τ and P values.

Site	Start year	End year	No. of years	M-K trend (τ)	M-K trend (P value)	M-K trend (τ for recent 20 years)	M-K trend (P value for recent 20 years)
CCEW	1985	2022	38	–0.02	0.85	–0.12	0.48
CHL	1976	2021	46	0.13	0.21	0.21	0.20
CPCR	1993	2021	29	–0.27	0.04	0.05	0.80
FRS	2004	2021	19	–0.19	0.28	–0.19	0.28
HBR	1956	2021	66	0.04	0.62	0.05	0.77
HJA	1957	2018	62	0.08	0.36	0.02	0.92
SAN	1977	2021	45	0.03	0.80	–0.09	0.58
SDEF	1975	2015	36	0.18	0.12	–0.20	0.23

Table 5.3. Results of trend analysis of annual maximum 24 h precipitation intensity including τ and P values.

Site	Start year	End year	No. of years	M-K trend (τ)	M-K trend (P value)	M-K trend (τ for recent 20 years)	M-K trend (P value for recent 20 years)
CCEW	1985	2022	38	0.03	0.81	0.11	0.54
CHL	1976	2021	46	0.26	0.01	0.16	0.35
CPCR	1993	2021	29	–0.24	0.07	0.22	0.18
FERN	1951	2022	72	0.03	0.67	–0.03	0.90
FRS	2004	2021	18	–0.06	0.76	–0.06	0.76
HBR	1956	2021	66	0.12	0.14	–0.02	0.92
HJA	1957	2018	62	–0.064	0.46	–0.28	0.08
MARC	1961	2022	62	–0.01	0.90	–0.20	0.23
SAN	1977	2021	45	0.13	0.22	0.08	0.63
SDEF	1975	2015	36	0.06	0.62	–0.11	0.52

5.4.3 Low-flow characteristics

The mean and variability of annual minimum 7-day average flow per unit drainage area (ANMIN7Q) for all sites are shown in Fig. 5.4. The SDEF, HBR and CCEW gauging stations recorded the lowest mean ANMIN7Q magnitudes of 0.0016, 0.002 and 0.004 l/s/ha. The annual variability of ANMIN7Q was relatively larger for the CHL and CPCR EFs. Trend analysis of long-term ANMIN7Q revealed a significant increase in the HBR and SDEF sites, and a significant decline at the FRS site (Fig. S5.4, and Table 5.5). During the last two decades, a significant positive trend was evident at the CHL and CPCR sites. The CCEW and HJA sites showed a non-significant negative trend and positive trend, respectively, in the most recent decades, as well as over the long-term period.

Overall, the results of the trend analysis of climatic extremes for both the peak and low-flow extremes revealed mixed patterns across the sites in varying climatic zones (Table 5.1). These findings suggest that the response of peak

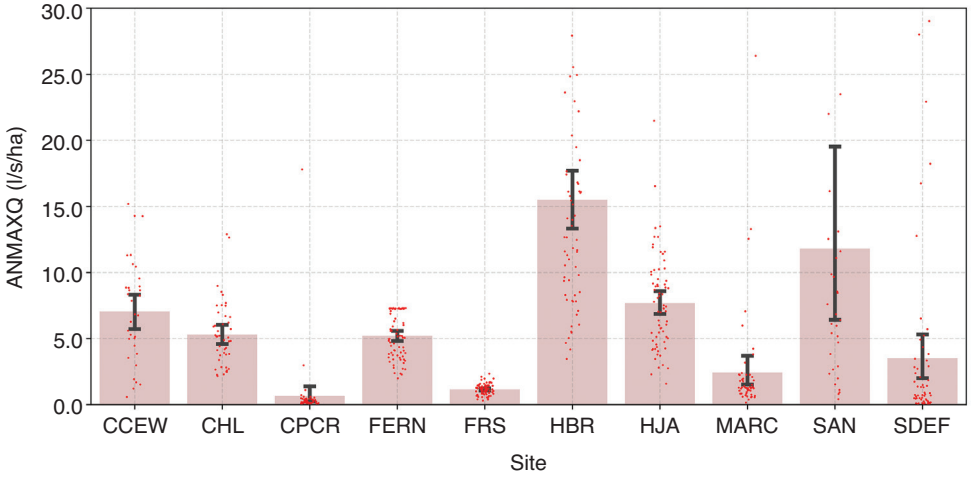

Fig. 5.3. Mean (box plots) and variability (1 SD, shown by whiskers) of annual maximum specific discharge (ANMAXQ, l/s/ha) for the selected study sites.

Table 5.4. Results of trend analysis of ANMAXQ including τ and P values.

Site	Start year	End year	No. of years	M-K trend (τ)	M-K trend (P value)	M-K trend (τ for recent 20 years)	M-K trend (P value for recent 20 years)
CCEW	1985	2017	33	–0.02	0.90	–0.18	0.28
CHL	1976	2020	45	0.06	0.58	0.00	1.00
CPCR	1969	2022	52	–0.05	0.61	–0.13	0.46
FERN	1951	2023	73	–0.13	0.10	–0.13	0.45
FRS	1943	2021	78	–0.03	0.73	0.34	0.04
HBR	1958	2021	64	0.28	0.00	0.04	0.82
HJA	1952	2019	68	–0.08	0.34	–0.03	0.87
MARC	1962	2017	56	–0.07	0.45	–0.29	0.08
SAN	1969	2016	31	–0.03	0.81	0.15	0.38
SDEF	1938	2001	57	–0.05	0.62	–0.17	0.30

streamflow to PIs induced by climate change are complex and are influenced by site-specific factors, such as climate, land use and land cover changes, as well as watershed characteristics including storage dynamics (Berghuijs *et al.*, 2016; Wasko *et al.*, 2020). The trend analysis highlights the importance of considering precipitation and streamflow when assessing water resources in the context of climate change. While increasing precipitation may lead to increased water availability in some areas, it may also lead to more frequent and intense flooding events. Understanding the trends in both precipitation and streamflow is crucial for developing effective water-management strategies that can adapt to changing climate, conditions. Understanding of the response of streams to precipitation inputs is still limited especially in northern headwater catchments (Tetzlaff *et al.*, 2013). Ali *et al.* (2015) published runoff initiation thresholds

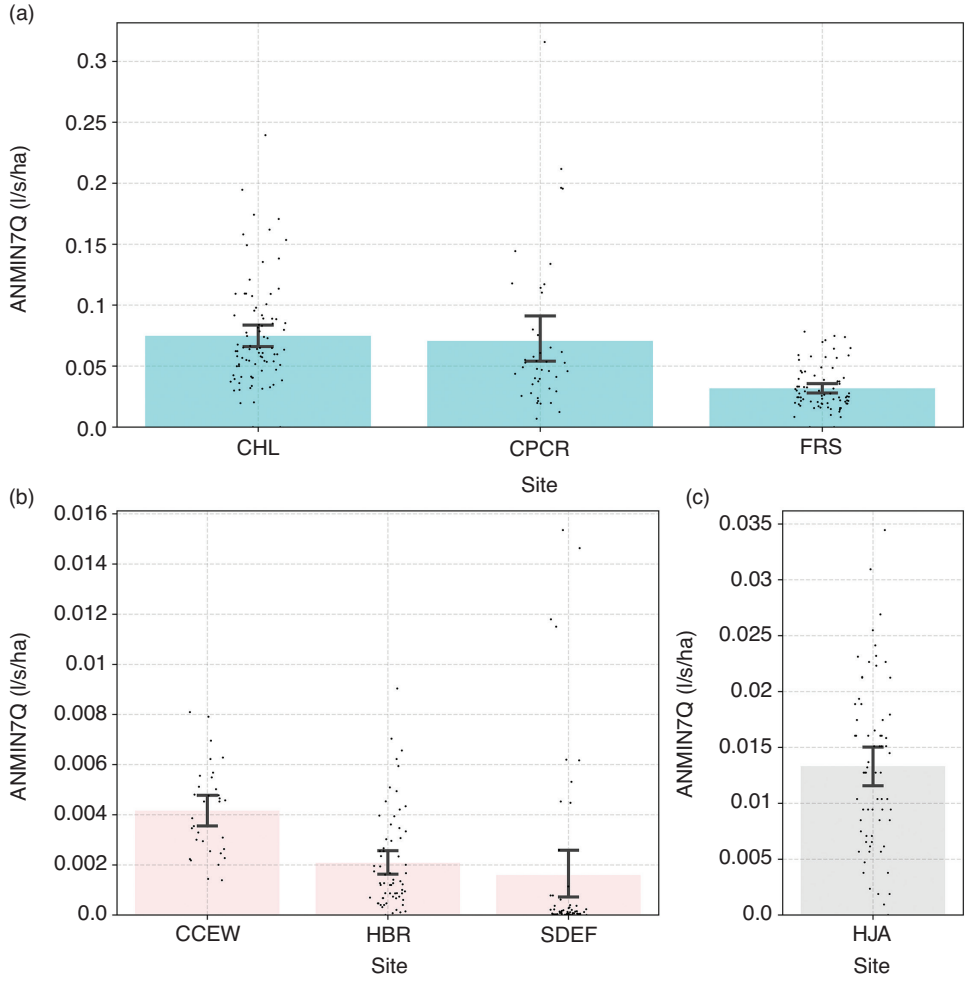

Fig. 5.4. (a–c) Mean (box plots) and variability (1 SD, shown by whiskers) of annual minimum 7-day average specific discharge (ANMIN7Q, l/s/ha) for the selected study sites.

and effective precipitation input thresholds for rainfall- and snowmelt-driven events for nine northern forested catchments that included HBR and HJA.

5.4.4 PIDF

The results of the frequency analysis of 1 and 24 hour PI for the selected sites are shown in Fig. 5.5 and Table S5.1. The results indicated that there was considerable variation in the magnitude and uncertainty of 1 and 24 hour PI values across different locations and return intervals. The mean 24 hour PI estimates for the 25-, 50- and 100 year return intervals ranged from 0.164 to 0.972 cm/h, 0.182 to 1.181 cm/h and 0.201 to 1.425 cm/h, respectively. SAN and CHL had the highest PI estimates for both durations and all return intervals, indicating that they experienced the most intense rainfall events. For example, the mean PI estimate for the 100 year

Table 5.5. Results of trend analysis of ANMIN7Q including τ and P values.

Site	Start year	End year	No. of years	M-K trend (τ)	M-K trend (P value)	M-K trend (τ for recent 20 years)	M-K trend (P value for recent 20 years)
CCEW	1985	2017	33	–0.16	0.18	–0.30	0.06
CHL	1936	2021	86	–0.04	0.60	0.41	0.01
CPCR	2012	2022	43	0.17	0.12	0.45	0.01
FRS	1943	2021	78	–0.25	0.00	–0.13	0.44
HBR	1957	2022	66	0.21	0.01	–0.02	0.95
HJA	1959	2019	68	0.14	0.09	–0.01	0.97
SDEF	1938	2001	57	0.31	0.00	–0.21	0.21

return interval for SAN was 0.972 cm/h for the 24 hour PI and 9.492 cm/h for the 1 hour PI, which were more than four times higher than the FRS mean PI estimates of 0.201 cm/h and 2.939 cm/h, respectively. However, they also had the widest CIs, suggesting that there was a high degree of uncertainty in the PI estimates for these sites. The 95% CIs for the 100 year return interval for SAN were 0.680–2.169 and 7.115–11.868 cm/h for the 24 and 1 hour PI, respectively.

In contrast, the FRS and CCEW sites had the lowest PI estimates for both durations and all return intervals, indicating that they had the least intense rainfall events. They also had the narrowest CIs, suggesting that there was a low degree of uncertainty in the PI estimates for these sites. The 95% CIs for the 100 year return interval for FRS were 0.080–0.323 and 1.705–4.173 cm/h for the 24 and 1 hour PI, respectively. This low degree of uncertainty could be due to the availability of data, the homogeneity of the terrain, or the stability of the climatic and hydrological conditions. The other sites (CPCR, HBR, HJA and SDEF) had intermediate PI estimates and CIs.

These results are consistent with previous findings (Amatya *et al.*, 2021; Mukherjee *et al.*, 2023) and provide important information for the design and management of water resources and infrastructure, as well as for the assessment and mitigation of flood risks. The PI estimates and CIs can be used to estimate the design storm for each site, which is the rainfall event with a specified return interval that is used as the basis for hydrological and hydraulic calculations. The design storm can help determine the capacity and performance of drainage systems, culverts and other road–stream crossing structures (Rosenzweig *et al.*, 2019). The results can also help identify the areas that are more prone to flooding and the factors that contribute to the uncertainty of the PI estimates. These results can inform the development of adaptation and resilience strategies to cope with the potential impacts of extreme rainfall events.

5.4.5 High-flow quantiles

The mean estimates of 25-, 50- and 100-year return intervals of annual maximum peak flow (ANMAXQ) per unit area along with their 95% upper and lower bounds, as a measure of the uncertainties for each of the sites, are shown in Fig. 5.6 and Table S5.2. The results suggested that the sites have different values of high-flow-specific discharges and different degrees of uncertainty.

The SAN site had the highest mean estimate of ANMAXQ for all the return intervals, indicating that it is prone to more severe floods than the other sites. For the 100-year return interval, the mean estimate was 107.2 l/s/ha, with a lower bound of 101.3 l/s/ha and an

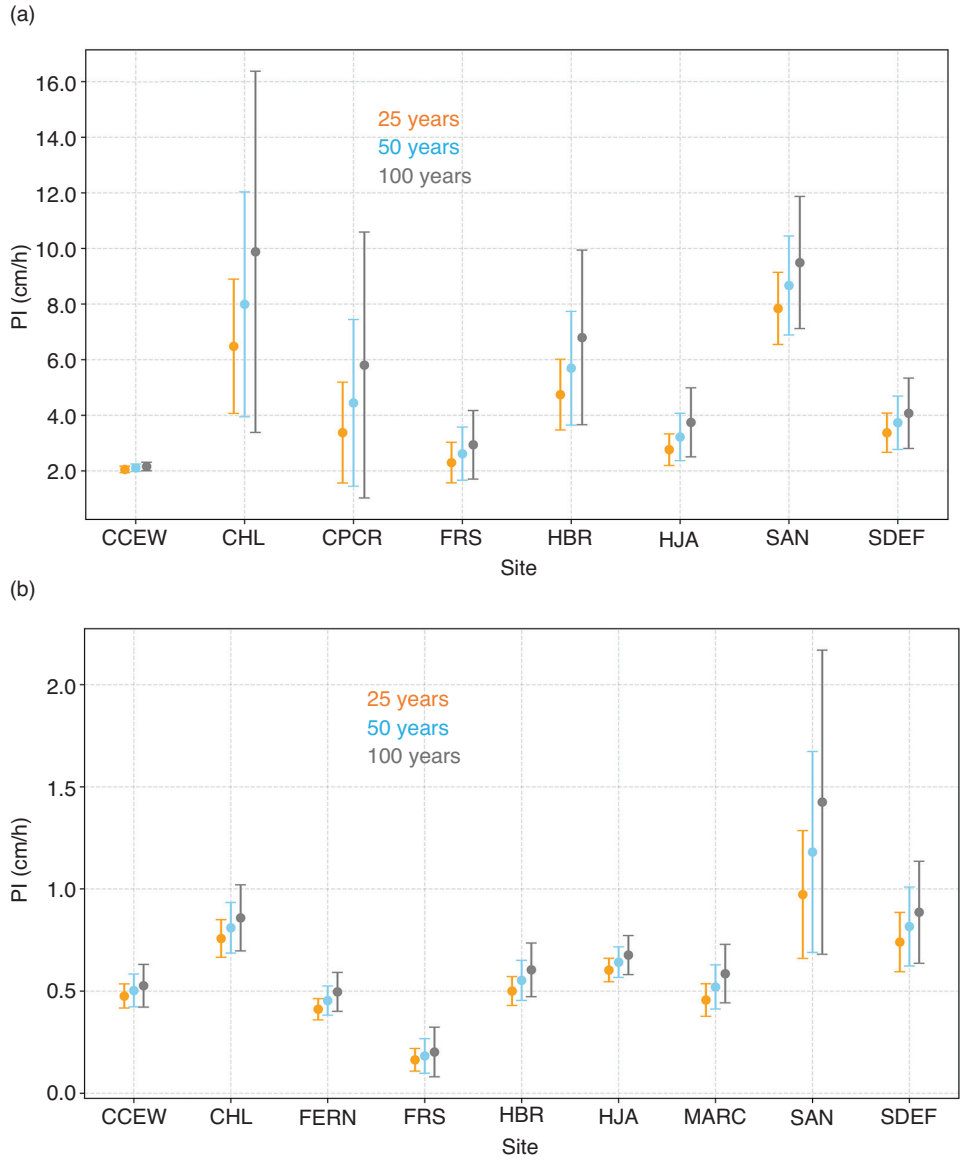

Fig. 5.5. (a) 1 hour and (b) 24 hour PI with 25-, 50- and 100-year events derived from the on-site rain gauge data for all sites. The error-bar plots show the estimates (filled circle) and 95% confidence bounds (error bars). Note that 1 hour PI results were not available for the FERN and MARC sites and therefore are not shown.

upper bound of 113.0 l/s/ha. SDEF had the widest CI for all the return intervals, indicating that it has the most uncertainty in the estimation of ANMAXQ. For the 100-year return interval, the mean estimate was 115.8 l/s/ha, with a lower bound of 97.7 l/s/ha and an upper bound of 133.8 l/s/ha. This means that the true value of ANMAXQ could be anywhere between 97.7 and 133.8 l/s/ha, which is a large range of variation. The FRS site had the lowest mean

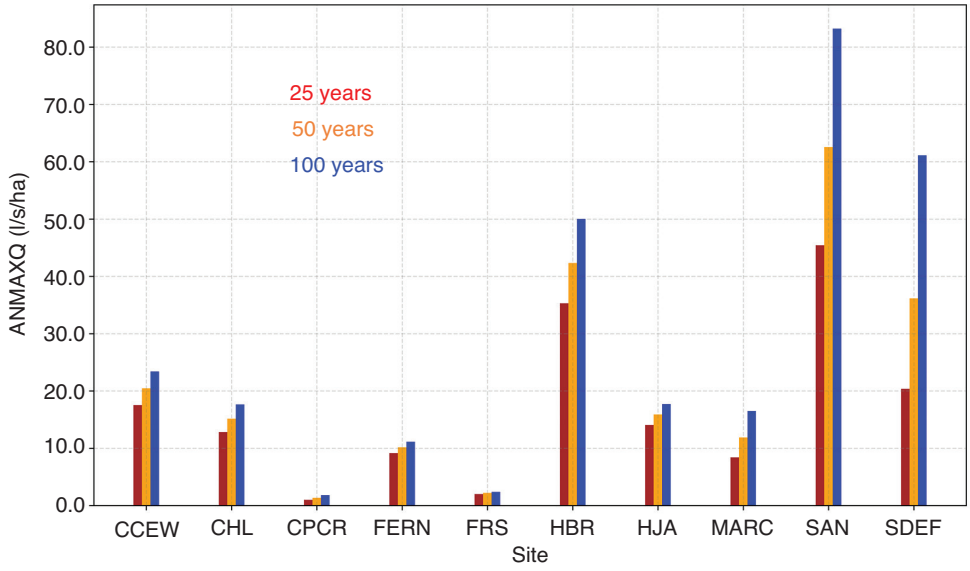

Fig. 5.6. Results for 25-year, 50-year and 100-year peak flow discharge per unit area (ANMAXQ in l/s/ha) for the selected stream gauges.

estimate of ANMAXQ and the narrowest CIs, indicating that it has the least risk of flooding and the most reliable estimation of ANMAXQ. For the 100-year return interval, the mean estimate was 2.2 l/s/ha, with a lower bound of 2.0 l/s/ha and an upper bound of 2.3 l/s/ha. The HBR site had a mean estimate of ANMAXQ for all the return intervals, indicating that it also has a high risk of flooding. For the 100-year return interval, the mean estimate was 66.5 l/s/ha, with a lower bound of 65.3 l/s/ha and an upper bound of 67.7 l/s/ha.

The HJA site had a relatively lower mean estimate of ANMAXQ compared with the HBR, SAN and SDEF sites, indicating that it also has a moderate risk of flooding and a reliable estimation of ANMAXQ. For the 100-year return interval, the mean estimate was 36.2 l/s/ha, with a lower bound of 36.0 l/s/ha and an upper bound of 36.4 l/s/ha. CCEW had a similar mean estimate of ANMAXQ for all the return intervals, indicating that it has a moderate risk of flooding. For the 100-year return interval, the mean estimate was 22.3 l/s/ha, with a lower bound of 21.9 l/s/ha and an upper bound of 22.8 l/s/ha. At the CHL site, the mean estimate of the 100-year return interval was 13.9 l/s/ha, with a lower bound of 13.6 l/s/ha and an upper bound of 14.2 l/s/ha.

Both the MARC and FERN sites had a low to moderate risk of flooding and fairly reliable estimations of ANMAXQ with quite similar mean estimates of 9.0 l/s/ha and 9.6 l/s/ha, respectively, for the 100-year return interval, with a slightly wider range of bounds for MARC than for FERN. The CPCR site, with a mean estimate is 3.6 l/s/ha, a lower bound of 3.5 l/s/ha and an upper bound of 3.8 l/s/ha for the 100-year return interval has a low risk of flooding but a very uncertain estimation of ANMAXQ.

The lower and upper bounds of the 95% CIs provide valuable information about the uncertainty associated with the estimated peak flow discharges. These intervals indicate a range within which the true discharge values are likely to fall, with 95% confidence. Sites like FERN, MARC and CHL exhibited relatively narrow CIs across all return periods, suggesting higher confidence in their discharge estimations. However, sites like SAN, CCEW and HBR had wider CIs, indicating greater uncertainty in their discharge estimations.

Overall, the results are consistent with previous studies (Amatya *et al.*, 2021; Mukherjee *et al.*, 2024) and can be used in forest road-culvert design to prevent failures caused by flooding. The high-flow quantiles can be used by engineers and land managers to reduce both economic and societal burdens through decreased failure rates, minimized maintenance costs and preserved ecological values within forested watersheds. However, meticulous selection of the most suitable design strategy remains paramount for both new and renovated road-crossing structures, including site inspections associated with identifying the geomorphological and post-wildfire flood vulnerabilities. Equally crucial is meticulous installation procedures, including alignment checks, stream dimension verification and thorough substrate composition assessment (Hansen *et al.*, 2009). Finally, implementation of effective monitoring protocols and strategies for the drainage culverts will ensure sustained flood resilience throughout their lifespan. In addition, the high flood quantiles can also have impacts on the carrying capacities of long-term gauging stations. For example, Amatya *et al.* (2016a) found some of the SAN gauging stations inundated with flows exceeding the established rating curve after the extreme rainfall of Hurricane Joaquin (3–4 October 2015) when over 590 mm of precipitation fell in 48 hour (Figs 5.2, 5.3 and 5.6) causing sustained ponding.

5.4.6 Low-flow quantiles

The results in Table 5.6 and Fig. 5.7 show the low-flow quantiles in L/s, with 95% confidence bounds, estimated using the annual minimum of 7-day average streamflow data for the six sites.

7Q10 varied across the sites, highlighting the heterogeneity of low-flow conditions in forested watersheds due to climate and precipitation patterns. The low-flow estimates at the SDEF site across all return intervals ranged from 0.0032 l/s/ha (5th percentile) to 0.0036 l/s/ha (95th percentile) for a 25-year return interval and from 0.1044 l/s/ha (5th percentile) to 0.1308 l/s/ha (95th percentile) for a 100-year return interval, reflecting the relatively stable precipitation pattern of this site. Similar to SDEF, the HJA site exhibited a stable low-flow uncertainty.

Among our ten sites, CHL and CPCR demonstrated the highest 10-year low flow of 0.127 and 0.124 l/s/ha, respectively (Table 5.6). This low 7Q10 suggests a low susceptibility to drought and minimal ecological stress during low-flow periods. CCEW exhibited moderately low 7Q10 magnitudes (Table 5.6) with a 10-year low flow of 0.18 l/s/ha. This value indicates a less-permanent flow regime, where the stream may become discontinuous during drought periods, as was observed in 2021 (Keppeler *et al.*, 2024). Typical of California, the CCEW aquatic ecosystem experiences seasonal drought, and stream organisms are adapted to more limited summer habitats. Water-resource managers regulate withdrawal and consumptive use during the low-flow season. Overall, this analysis highlights the diverse flow characteristics across the ten sites. While some sites exhibited consistent and predictable flow regimes, others presented more complex patterns requiring further investigation, particularly SDEF's potential transition from intermittent to perennial flow. By analyzing low-flow statistics, ecologists can quantify the potential impacts of low-flow events on forest health and productivity. For example, declining fall precipitation has reduced fall flows, thereby impeding salmonid spawning migration in northern California (Keppeler *et al.*, 2024). This information enables the development of data-driven management strategies to mitigate low-flow stress on ecosystems and prioritize conservation efforts for vulnerable watersheds. Ultimately, this approach ensures the sustainable management and conservation of forested landscapes in the face of changing climatic conditions.

5.5 Conclusions

This study was conducted using long-term measured high-resolution annual maximum PIs and extreme high and low streamflow rates from ten USDA Forest Service EFs. We first evaluated the long-term temporal characteristics and trends of hydrometeorological variables, assuming their stationarity, followed by a cross-site comparison

Table 5.6. Minimum 7-day flow (ANMIN7Q) for 2-, 5-, 10-, 25-, 50- and 100-year return intervals (RIs) with lower and upper 95% confidence intervals (bounds) (l/s/ha).

Site	RI (years)	Non-exceedance probability	Estimates	Lower bound	Upper bound
CCEW	2	0.5	0.10	0.10	0.10
	5	0.8	0.15	0.15	0.15
	10	0.9	0.18	0.18	0.18
	25	0.96	0.23	0.23	0.23
	50	0.98	0.26	0.26	0.267
	100	0.99	0.30	0.29	0.31
CHL	2	0.5	0.066	0.066	0.066
	5	0.8	0.102	0.102	0.102
	10	0.9	0.128	0.127	0.129
	25	0.96	0.164	0.162	0.166
	50	0.98	0.193	0.191	0.194
	100	0.99	0.223	0.221	0.226
CPCR	2	0.5	0.053	0.052	0.054
	5	0.8	0.093	0.092	0.094
	10	0.9	0.126	0.124	0.128
	25	0.96	0.175	0.171	0.178
	50	0.98	0.217	0.212	0.221
	100	0.99	0.264	0.257	0.271
FRS	2	0.5	0.028	0.028	0.028
	5	0.8	0.045	0.044	0.045
	10	0.9	0.057	0.057	0.057
	25	0.96	0.075	0.075	0.076
	50	0.98	0.090	0.089	0.091
	100	0.99	0.106	0.105	0.108
HBR	2	0.5	0.0012	0.0012	0.0014
	5	0.8	0.0028	0.0028	0.0028
	10	0.9	0.0042	0.0042	0.0042
	25	0.96	0.0064	0.0064	0.0064
	50	0.98	0.0083	0.0080	0.0083
	100	0.99	0.0101	0.0099	0.0104
HJA	2	0.5	0.0010	0.0010	0.0010
	5	0.8	0.0023	0.0022	0.0023
	10	0.9	0.0033	0.0033	0.0033
	25	0.96	0.0048	0.0047	0.0048
	50	0.98	0.0060	0.0060	0.0062
	100	0.99	0.0073	0.0072	0.0075
SDEF	2	0.5	0.0000	0.0000	0.0000
	5	0.8	0.0012	0.0008	0.0012

Continued

Table 5.6. Continued

Site	RI (years)	Non-exceedance probability	Estimates	Lower bound	Upper bound
	10	0.9	0.0032	0.0032	0.0036
	25	0.96	0.0140	0.0128	0.0152
	50	0.98	0.0408	0.0368	0.0452
	100	0.99	0.1176	0.1044	0.1308

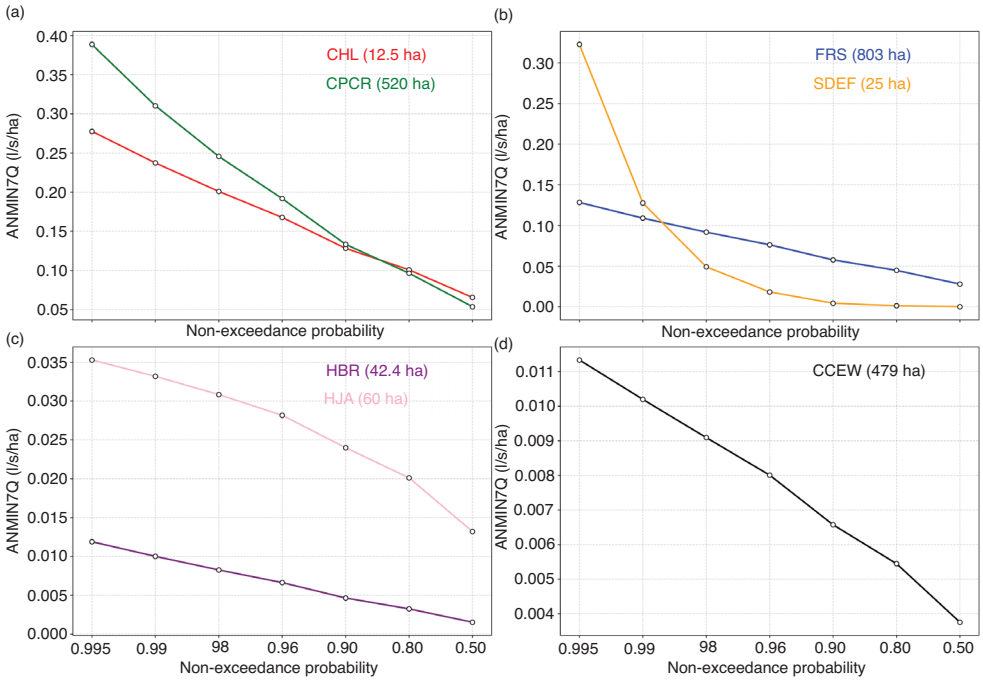

Fig. 5.7. Low-flow frequency curves for the annual minimum 7-day average streamflow per unit drainage area (ANMIN7Q, l/s/ha) for the selected stream gauges.

of the extreme (≥25 year return interval) PIDF and high (≥25 years) and low (≥10 years) flow frequencies of discharges. Frequencies of 25 years or more are commonly used in design of road cross-drainage and stormwater management structures and other similar ecological applications. Similarly, 10 year frequency low-flow quantiles are generally used in assessing environmental flows for aquatic ecosystems.

The results suggested that the SAN, CHL and HBR sites had the highest mean values and variability of 1 and 24 hour annual maximum PIs (ANMAXPI), while the FRS and CPCR sites had the lowest. Trend analysis suggested a significant ($\alpha = 0.05$) long-term decrease in 1 hour PI at the CPCR site and an increase in 24 hour PI at the CHL site. These results are consistent with the results of the PIDF analysis yielding the highest and most uncertain PIs for the 25-, 50- and 100 year return intervals at the CHL (for 1 hour) and SAN (for 24 hour) sites. The extreme high-flow characteristics and trend analysis indicated a similar complex spatiotemporal pattern across the sites, with the highest mean annual maximum specific discharge (ANMAXQ) at the low-gradient SAN site and the high-gradient HBR site, both on the east coast. A significant positive long-term trend of ANMAX was also found at the HBR site. A relatively high interannual variability of ANMAXQ at the SAN,

HBR and SDEF sites is also consistent with their higher 25-, 50- and 100 year ANMAXQ values than all other sites. In contrast, FRS and CPCR yielded the lowest risk of flooding based on their low 100 year ANMAXQ values. The other sites had intermediate values and uncertainties. Similarly, the assessment of extreme low-flow characteristics revealed that SDEF, HBR and CCEW had the lowest mean and variability of ANMIN7Q. Trend analysis revealed diverse temporal patterns of ANMIN7Q, with some sites showing long-term and recent temporal increases, some showing the opposite, and others showing divergent trends in the recent 20 year period. The extreme low-flow frequency analysis indicated the highest ANMIN7Q values of 0.127 and 0.124 l/s/ha at the CHL and CPCR sites, respectively, suggesting a low susceptibility to drought and minimal ecological stress during low-flow periods at these sites. In contrast, SDEF, situated in the dry chaparral of southern California, exhibited the lowest flow magnitude among all sites, with a 10 year low flow of 0.0016 l/s/ha.

Overall, the findings showed sites with different impacts of climate change and variability on streamflow regimes, and that site-specific factors, such as climate, land use and land cover changes, and watershed characteristics, play a role in determining the response of streams to precipitation inputs. Consistent with Wright *et al.* (2019), we believe that, although trends in rainfall extremes may not have necessarily translated into observable increases in flood risks, these results on extreme precipitation and flood frequencies none the less would be of use in hydrological design applications, taking into consideration recent changes in extreme rainfall properties at the USFS FE watersheds (Amatya *et al.*, 2016a; Amatya *et al.*, 2021; Mukherjee *et al.*, 2023; Mukherjee *et al.*, 2024). In addition, the derived flood frequencies from these reference watersheds may serve the purpose of comparing them with those from the paired treatment watersheds at these EFs to correctly evaluate the treatment effects as opposed to a chronologically paired approach, as argued by Alila *et al.* (2009).

Although this study has provided valuable insights into the trends and variability of hydrometeorological variables across ten USDA Forest Service EFs, and their implications for flood risk, water availability and ecological health, there are still some limitations and challenges that need to be addressed in future research. First, the assumption of stationarity may not be valid for some sites, especially under the influence of climate change and human activities. Therefore, alternative methods that account for non-stationarity (Cheng and AghaKouchak, 2014) may be more suitable for detecting and quantifying changes in hydrometeorological variables. Second, the data record availability and quality may result in high uncertainty, warranting a need for more data collection and quality control to improve the robustness of the results and reduce uncertainties. Third, the spatial and temporal scales of the analysis may influence the interpretation and application of the findings. For instance, the annual and seasonal trends may not capture the subseasonal or daily variations that are important for hydrological design and management, particularly the timing of occurrence of annual peak discharge relative to the timing of the precipitation intensities in these small headwater forest watersheds. Similarly, the site-specific factors may not reflect the regional or global patterns of climate change and variability. Even where data are available for relatively long periods (20–50 years) and the distribution of discharge is fairly well known, there is little confidence in estimates of high-flow discharges for return periods of over 50 years (Eisenbies *et al.*, 2007). Therefore, more comprehensive and multi-site and multi-scale analyses globally are needed to better understand the hydrometeorological processes and their interactive effects, as a result of climate change, on forest management of streamflow, particularly during extreme events, as was shown for the Coweeta watersheds (Kelly *et al.*, 2016), and the effects of extreme precipitation on hydrological behavior transformation in watersheds, as shown by Jayakaran *et al.* (2014).

References

Adams, M.B., Kochenderfer, J.N., Wood, F., Angradi, T.R. and Edwards, P.J. (1994) Forty Years of Hydrometeorological Data from the Fernow Experimental Forest. General Technical Report NE-184. Forest Service: Northeastern Forest Experiment Station.

Ali, G., Tetzlaff, D., McDonnell, J.J., Soulsby, C., Carey, S. *et al*. (2015) Comparison of threshold hydrologic response across northern catchments. *Hydrological Processes* 29, 3575–3591.

Alila, Y.P., Kuras, K., Schnorbus, M. and Hudson, R. (2009) Forests and floods: A new paradigm sheds light on age-old controversies. *Water Resources Research* 45, W08416.

Amatya, D.M., Harrison, C.A. and Trettin, C.C. (2016a) Hydro-meteorologic assessment of October 2015 extreme precipitation event on Santee Experimental Forest watersheds, South Carolina. *Journal of South Carolina Water Resources* 3, 19–30.

Amatya, D.M., Campbell, J., Wohlgemuth, P., Elder, K.E., Sebestyen, S. *et al*. (2016b) Hydrological processes of reference watersheds in experimental forests, USA. In: Amatya, D.M., Williams, T.M., Bren, L. and Jong, C. (eds) *Forest Hydrology: Processes, Management, and Applications*. CAB International, Wallingford, UK, pp. 219–239.

Amatya, D.M., Tian, S., Marion, D.A., Caldwell, P., Laseter, S. *et al*. (2021) Estimates of precipitation IDF curves and design discharges for road-crossing drainage structures: Case study in four small forested watersheds in the southeastern US. *Journal of Hydrologic Engineering* 26, 05021004.

Ansa Thasneem, S., Chithra, N.R. and Thampi, S.G. (2021) Assessment of nonstationarity and uncertainty in precipitation extremes of a river basin under climate change. *Environmental Modeling and Assessment* 26, 295–312.

Berghuijs, W.R., Woods, R.A., Hutton, C.J. and Sivapalan, M. (2016) Dominant flood generating mechanisms across the United States. *Geophysical Research Letters* 43, 4382–4390.

Blöschl, G., Hall, J., Viglione, A., Perdigão, R.A., Parajka, J. *et al*. (2019) Changing climate both increases and decreases European river floods. *Nature* 573, 108–111.

Bolton, W.R., Hinzman, L.D. and Yoshikawa, K. (2004) Water balance dynamics of three small catchments in a sub-Arctic boreal forest. In: Kane, D.L. and Yang, D. (eds) *Proceedings of a Northern Research Basins Water Balance Workshop, 15–19 March 2004, Victoria, BC*, International Association of Hydrological Sciences, Victoria, Canada, pp. 213–223.

Bonnin, G.M., Martin, D., Lin, B., Parzybok, T., Yekta, M. *et al*. (2006) *Precipitation-frequency atlas of the United States Vol. 1, Version 5.0: Semiarid Southwest (Arizona, Southeast California, Nevada, New Mexico, Utah*), NOAA Atlas 14. US Department of Commerce, Silver Spring, Maryland.

Burt, T.P., Miniat, C., Laseter, S.H. and Swank, W.T. (2018) Changing patterns of daily precipitation totals at the Coweeta Hydrologic Laboratory, North Carolina, USA. *International Journal of Climatology* 38, 94–104.

Cafferata, P.H. and Reid, L.M. (2013) *Application of long-term watershed research to forest management in California: 50 years of learning from Caspar Creek Experimental watersheds*. California Forestry Report No. 5. California: Natural Resources Agency, Department of Forestry and Fire Protection.

Campbell, J., Driscoll, C.T., Jones, J.A., Boose, E.R., Dugan, H.A. *et al*. (2022) Forest and freshwater ecosystem responses to climate change and variability at US LTER sites. *BioScience* 72, 851–870.

Campbell, J.L., Driscoll, C.T., Pourmokhtarian, A. and Hayhoe, K. (2011) Streamflow responses to past and projected future changes in climate at the Hubbard Brook Experimental forest, New Hampshire, USA. *Water Resources Research* 47, W02514.

Cheng, L. and AghaKouchak, A. (2014) Nonstationary precipitation intensity-duration-frequency curves for infrastructure design in a changing climate. *Scientific Reports* 4, 7093.

Coles, S., Bawa, J., Trenner, L. and Dorazio, P. (2001) *An Introduction to Statistical Modeling of Extreme Values*. Springer, London.

Cox, C. (1990) Fieller's theorem, the likelihood and the delta method. *Biometrics* 46, 709–718.

Daly, C., Schulze, M. and McKee, W. (2019) Meteorological data from benchmark stations at the HJ Andrews Experimental Forest, 1957 to present. Available at: https://andlter.forestry.oregonstate.edu/data/abstractdetail.aspx?dbcode=ms001 (accessed 17 April 2025).

de Luca, D. and Galasso, L. (2018) Stationary and non-stationary frameworks for extreme rainfall time series in Southern Italy. *Water* 10, 1477.

Dunn, P.H., Barro, S.C., Wells, W.G.I., Poth, M.A., Wohlegemuth, P.M. *et al*. (1988) *The San Dimas Experimental Forest: 50 Years of Research*. General Technical Report PSW-105. Berkeley, California: US Forest Service.

Eisenbies, M., Aust, W., Burger, J. and Adams, M.B. (2007) Forest operations, extreme flooding events, and considerations for hydrologic modeling in the Appalachians – A review. *Forest Ecology and Management* 242, 77–98.

England, J.F.J., Cohn, T.A., Faber, B.A., Stedinger, J.R., Thomas, W.O.J. *et al*. (2019) *Guidelines for Determining Flood Flow Frequency*, Bulletin 17C (No. 4-B5). US Geological Survey. Available at: www.usgs.gov/publications/guidelines-determining-flood-flow-frequency-bulletin-17c (accessed 17 April 2025).

Feaster, T.D. and Guimaraes, W.B. (2014) Low-flow Frequency and Flow Duration of Selected South Carolina Streams in the Catawba-Wateree and Santee River Basins through March 2012. US Geological Survey Open-File Report 2014-1113. Available at: https://pubs.usgs.gov/publication/ofr20141113 (accessed 17 April 2025).

Feaster, T.D., Gotvald, A.J. and Weaver, J. (2009) *Magnitude and Frequency of Rural Floods in the Southeastern United States, 2006: Volume 3, South Carolina*. US Geological Survey. Available at: https://pubs.usgs.gov/publication/sir20095156 (accessed 17 April 2025).

Gimeno, L., Sorí, R., Vazquez, M., Stojanovic, M., Algarra, I. *et al*. (2022) Extreme precipitation events. *WIREs Water* 9, e1611.

Gu, X., Zhang, Q., Singh, V.P. and Shi, P. (2017) Nonstationarity in timing of extreme precipitation across China and impact of tropical cyclones. *Global Planet Change* 149, 153–165.

Haan, C.T., Barfield, B.J. and Hayes, J.C. (1994) *Design Hydrology and Sedimentology for Small Catchments*. Elsevier, London.

Hamon, W.R. (1963) Estimating potential evapotranspiration. *Journal of the Hydraulics Division* 87, 107–120.

Hansen, B., Nieber, J.L. and Lenhart, C. (2009) *Cost analysis of alternative culvert installation practices in Minnesota*. University of Minnesota Digital Conservancy, Minnesota.

Hargreaves, G.H. and Samani, Z.A. (1982) Estimating potential *evapotranspiration*. *Journal of Irrigation and Drainage Division* 108, 223–230.

Heredia, N., Roper, B., Gillespie, N. and Roghair, C. (2016) *Technical Guide for Field Practitioners: Understanding and Monitoring Aquatic Organism Passage at Road Stream Crossings*. Technical Report no.TR-101. Center, USDA. Washington, DC: Forest Service, National Stream and Aquatic Ecology.

Hook, D.D., Buford, M.A. and Williams, T.M. (1991) Impact of hurricane hugo on the South Carolina coastal pine forest. *Journal of Coastal Research SI* 291–300.

Interagency Advisory Committee on Water Data (1982) *Guidelines for Determining Flood Flow Frequency – Bulletin 17B of the Hydrology Subcommittee*. US Geological Survey, Office of Water Data Coordination, Reston, Virginia.

Jalowska, A.M., Spero, T.L. and Bowden, J.H. (2021) Projecting changes in extreme rainfall from three tropical cyclones using the design rainfall approach. *Npj Climate and Atmospheric Science* 4, 23.

Jayakaran, A., Williams, T.M., Ssegane, H.S., Amatya, D.M., Song, B. *et al*. (2014) Hurricane impacts on a pair of coastal forested watersheds: Implications of selective hurricane damage to forest structure and streamflow dynamics. *Hydrology and Earth System Science* 18, 1151–1164.

Jian, X., Wolock, D.M., Jenter, H.L. and Brady, S. (2015) *Streamflow of 2014: Water Year Summary*, Fact Sheet No. 2015-3026. US Geological Survey. Available at: https://pubs.usgs.gov/fs//2015/3026/ (accessed 17 April 2025).

Johnson, S., Henshaw, D., Downing, G., Wondzell, S., Schulze, M. *et al*. (2021) Cascade Mountains, Oregon. *Hydrological Processes* 35, e14187.

Johnson, S., Wondzell, S. and Rothacher, J. (2023) Stream discharge in gaged watersheds at the HJ Andrews Experimental Forest, 1949 to present. Available at: https://andlter.forestry.oregonstate.edu/data/abstractdetail.aspx?dbcode=hf004 (accessed 17 April 2025).

Jones, J.B. and Rinehart, A.J. (2010) The long-term response of stream flow to climatic warming in headwater streams of interior Alaska. *Canadian Journal of Forest Research* 40, 1210–1218.

Kelly, C.N., McGuire, K.J., Miniat, C.F. and Vose, J.M. (2016) Streamflow response to increasing precipitation extremes altered by forest management. *Geophysical Research Letters* 43, 3727–3736.

Kendall, M.G. (1975) *Rank Correlation Methods*, 4th edn. Charles Griffin, London.

Keppeler, E., Wagenbrenner, J., Dymond, S. and Dralle, D. (2024) Streamflow response to drought in a managed coast redwood catchment. *Journal of the American Water Resources Association* 60, 928–952.

Kim, H., Kim, S., Shin, H. and Heo, J.H. (2017) Appropriate model selection methods for nonstationary generalized extreme value models. *Journal of Hydrology* 547, 557–574.

Laio, F. (2004) Cramer–von Mises and Anderson–Darling goodness of fit tests for extreme value distributions with unknown parameters. *Water Resources Research* 40, W09308.

Laseter, S.H., Ford, C.R., Vose, J.M. and Swift, L.W. (2012) Long-term temperature and precipitation trends at the Coweeta Hydrologic Laboratory, Otto, North Carolina, USA. *Hydrology Research* 43, 890–901.

Mann, H.B. (1945) Non-parametric tests against trend. *Econometrica* 13, 163–171.

Martins, E.S. and Stedinger, J.R. (2000) Generalized maximum-likelihood generalized extreme-value quantile estimators for hydrologic data. *Water Resources Research* 36, 737–744.

Meixner, T. and Wohlgemuth, P.M. (*et al*2003) Climate variability, fire, vegetation recovery, and watershed hydrology. In: Renard, K.G., McElroy, S.A., Gburek, W.J., Canfield, H.E., Russell, L. et al. (eds) *The First Interagency Conference on Research in the Watersheds*, Benson, Arizona, October 27–30, 2003, pp. 651–656.

Milly, P.C., Betancourt, J., Falkenmark, M., Hirsch, R.M., Kundzewicz, Z.W. *et al*. (2008) Stationarity is dead: Whither water management. *Science* 319, 573–574.

Mukherjee, S., Amatya, D.M., Jalowska, A., Campbell, J.L., Johnson, S.L. *et al*. (2023) Comparison of on-site versus NOAA's extreme precipitation intensity-duration-frequency estimates for six forest headwater catchments across the continental United States. *Stochastic Environmental Research and Risk Assessment* 37, 4051–4070.

Mukherjee, S., Amatya, D.M., Campbell, J.L., Gryczkowski, L., Panda, S. *et al*. (2024) A watershed-scale multi-approach assessment of design flood discharge estimates used in hydrologic risk analyses for forest road stream crossings and culverts. *Journal of Hydrology* 632L, 130698.

National Research Council (1988) *Estimating Probabilities of Extreme Floods – Methods and Recommended Research*. National Academy Press, Washington, DC.

National Research Council (1995) *Flood Risk Management and The American River Basin; an Evaluation*. National Academy Press, Washington, DC.

Nerantzaki, S.D. and Papalexiou, S.M. (2022) Assessing extremes in hydroclimatology: A review on probabilistic methods. *Journal of Hydrology* 605, 127302.

Papalexiou, S.M. and Montanari, A. (2019) Global and regional increase of precipitation extremes under global warming. *Water Resources Research* 55, 4901–4914.

Patric, J.H. and Goswami, N. (1968) Evaporation pan studies – forest research at Parsons. *West Virginia Agriculture and Forestry* 1, 6–10.

Peel, M.C., Finlayson, B.L. and McMahon, T.A. (2007) Updated world map of the Köppen-Geiger climate classification. *Hydrology and Earth System Sciences* 11, 1633–1644.

Perica, S., Martin, D., Pavlovic, S., Roy, I., Laurent, M. *et al*. (2013) *NOAA Atlas 14 Precipitation-Frequency Atlas of the United States*. National Oceanic and Atmospheric Administration, Silver Spring, Maryland.

Perica, S., Pavlovic, S., Laurent, M., Trypaluk, C., Unruh, D. *et al*. (2018) Precipitation-Frequency Atlas of the United States. Version 2.0. Texas (Vol. 11). Texas: National Oceanic Atmospheric Administration.

Preece, J.R., Shinker, J.J., Riebe, C.S. and Minckley, T.A. (2021) Elevation-dependent precipitation response to El Niño-Southern Oscillation revealed in headwater basins of the US Central Rocky Mountains. *International Journal of Climatology* 41, 1199–1210.

Richardson, P.W., Seehafer, J.E., Keppeler, E.T., Sutherland, D.G. and Wagenbrenner, J.W. (2021) Fifty-eight years and counting of watershed science at the Caspar Creek experimental watersheds in Northern California. *Hydrological Processes* 35, e14207.

Riggs, H.C. (1985) *Streamflow Characteristics*. Elsevier, Amsterdam, Netherlands.

Rosenzweig, B., Ruddell, B.L., McPhillips, L., Hobbins, R., McPhearson, T. *et al*. (2019) Developing knowledge systems for urban resilience to cloudburst rain events. *Environmental Science and Policy* 99, 150–159.

Rothacher, J., Dyrness, C.T. and Fredriksen, R.L. (1967) *Hydrologic and Related Characteristics of Three Small Watersheds in the Oregon Cascades*. Pacific Northwest Forest and Range Experiment Station, Forest Service, US Department of Agriculture, Portland, Oregon.

Salas, J., Obeysekera, J. and Vogel, R. (2018) Techniques for assessing water infrastructure for nonstationary extreme events: A review. *Hydrologic Sciences Journal* 63, 325–352.

Sebestyen, S.D., Dorrance, C., Olson, D.M., Verry, E.S., Kolka, R.K. *et al*. (2011) Long-term monitoring sites and trends at the Marcell Experimental Forest. In: Kolka, R.K., Sebestyen, S.D., Verry, E.S. and Brooks, K.N. (eds) *Peatland Biogeochemistry and Watershed Hydrology at The Marcell Experimental Forest*. CRC Press, Boca Raton, Florida, pp. 15–71.

Sebestyen, S.D., Lany, N.K., Roman, D.T., Burdick, J.M., Kyllander, R.L. *et al*. (2021) Hydrological and meteorological data from research catchments at the Marcell Experimental Forest, Minnesota, USA. *Hydrologic Processes* 35, e14092.

Sen, P.K. (1968) Estimates of the regression coefficient based on Kendall's tau. *Journal of the American Statistical Association* 63, 1379–1389.

Sharma, A., Wasko, C. and Lettenmaier, D.P. (2018) If precipitation extremes are increasing, why aren't floods? *Water Resources Research* 54, 8545–8551.

Srivastava, A., Grotjahn, R., Ullrich, P.A. and Risser, M. (2019) A unified approach to evaluating precipitation frequency estimates with uncertainty quantification: Application to Florida and California watersheds. *Journal of Hydrology* 578, 124095.

Sun, G., Tiwari, K.R., Hao, L., Amatya, D., Liu, N. *et al*. (2023) Climate change and forest hydrology in future forests. In: McNulty, S.G. (ed.) *Future Forests: Mitigation and Adaptation to Climate Change*. Elsevier, Amsterdam, Netherlands, pp. 95–124.

Tetzlaff, D., Carey, S. and Soulsby, C. (2013) Catchments in the future North: Interdisciplinary science for sustainable management in the 21st century. North-Watch Workshop, Potsdam, Germany, 21–25 May 2012, *Hydrological Processes* 27, 635–774.

Thornthwaite, C.W. (1948) An approach toward a rational classification of climate. *Geographical Review* 38, 55–94.

USGS (1982) *Guidelines for Determining Flood Frequency*. Bulletin 17B of the Hydrology Subcommittee. Revised September 1981, Editorial Corrections, March 1982. US Department of Interior Geological Survey, Reston, Virginia.

van Cleve, K., Chapin, F.S., Ruess, R., Mack, M.C., Jones, J.B. *et al*. (2023) *Caribou-Poker Creeks Research Watershed: Daily Flow Rates for C2, C3, C4*. Version 24. Environmental Data Initiative.

Verry, E.S., Brooks, K.N., Nichols, D.S., Ferris, D.R. and Sebestyen, S.D. (2011) Watershed hydrology. In: Kolka, R.K., Sebestyen, S.D., Verry, E.S. and Brooks, K.N. (eds) *Peatland Biogeochemistry and Watershed Hydrology at the Marcell Experimental Forest*. CRC Press, Boca Raton, Florida, pp. 193–212.

Wang, H. and Sun, F. (2020) On the stationarity of annual precipitation over China (1959–2018). *Journal of Hydrometeorology* 21, 881–890.

Wasko, C., Nathan, R. and Peel, M.C. (2020) Trends in global flood and streamflow timing based on local water year. *Water Resources Research* 56, e2020WR027233.

Wohlgemuth, P.M. (2016) Long-term hydrologic research on the San Dimas Experimental Forest: Lessons learned and future directions. In: *Proceedings of the 5th Interagency Conference on Research in the Watersheds*, General Technical Report GTR-SRS-xxx. Southern Research Station, US Department of Agriculture, Forest Service, Ashville, North Carolina.

Wondzell, S.M. and Swanson, F.J. (1999) Floods, channel change, and the hyporheic zone. *Water Resources Research* 35, 555–567.

Wright, D.B., Bosma, C.D. and Lopez-Cantu, T. (2019) US hydrologic design standards insufficient due to large increases in frequency of rainfall extremes. *Geophysical Research Letters* 46, 8144–8153.

Yochum, S.E., Scott, J.A. and Levinson, D.H. (2019) Methods for assessing expected flood potential and variability: Southern Rocky Mountains region. *Water Resources Research* 55, 6392–6416.

Forest Hydrology

2ND EDITION

PROCESSES, MANAGEMENT AND ASSESSMENT

Edited by **Leon J. Bren, Devendra M. Amatya, Thomas M. Williams, Carmen de Jong** and **Ge Sun**

Forests cover about a third of the world's land surface area. They represent a distinct biotic community, provide a living for many millions of people, and provide fresh water to sustain communities. Forests capture part of the precipitation and pass the remainder into the soil. Some of this is then passed back to the atmosphere along with some to streams as a regulated outflow. Forest cover is generally the preferred land-use for clean water supplies, recreation, tourism, and other ecosystem benefits around the world. In many cases the value of the water exceeds the value of other forest products.

The discipline "forest hydrology" was developed in the 19th and 20th Century with the aim of putting such water cycling processes into a scientific framework incorporating forest watershed management. The 21st Century has seen proliferations of new technologies that have changed society, our living environment, and this discipline. Forests are also facing unprecedented threats from land conversion, fire, drought, and the changing climate. The discipline of forest hydrology must address these issues with innovation and new ideas.

The 2nd Edition of Forest Hydrology:

- Presents advances of understanding of key forest hydrologic processes (particularly evapotranspiration)
- Presents cutting-edge thinking and assessments in global forest hydrology, including state-of-the-art modelling and methodologies
- Presents innovative findings about the impacts of forest fires on the rate of catchment formation and how past fires have led to the catchments we take for granted
- Describes the latest challenges facing forest hydrology, such as increased occurrences of disturbance due to extreme precipitation and floods, drought, disease, fire, and their association with climate change
- Reviews the latest perceptions of the value of forested catchments compared to alternatives such as desalination plants
- Is written by an internationally renowned team of scientists, engineers, and forest managers to give a well-rounded view of the subject

This book is essential reading for graduate students, professionals, land managers, practitioners, and researchers with a good understanding of the basic principles of hydrology and hydrologic processes.

Front cover image: Forests provide clean water in the humid Southern Appalachian Mountains, one of world 'Hot spots' of biodiversity. Photo taken in the Linville Gorge Wilderness Area, the Pisgah National Forest in western North Carolina, USA. October 21, 2023 by Ge Sun

Forest Hydrology
PROCESSES, MANAGEMENT AND ASSESSMENT
2ND EDITION

Bren
Amatya
Williams
de Jong
Sun

Forest Hydrology
2ND EDITION
PROCESSES, MANAGEMENT AND ASSESSMENT
Edited by **Leon J. Bren, Devendra M. Amatya, Thomas M. Williams, Carmen de Jong** and **Ge Sun**

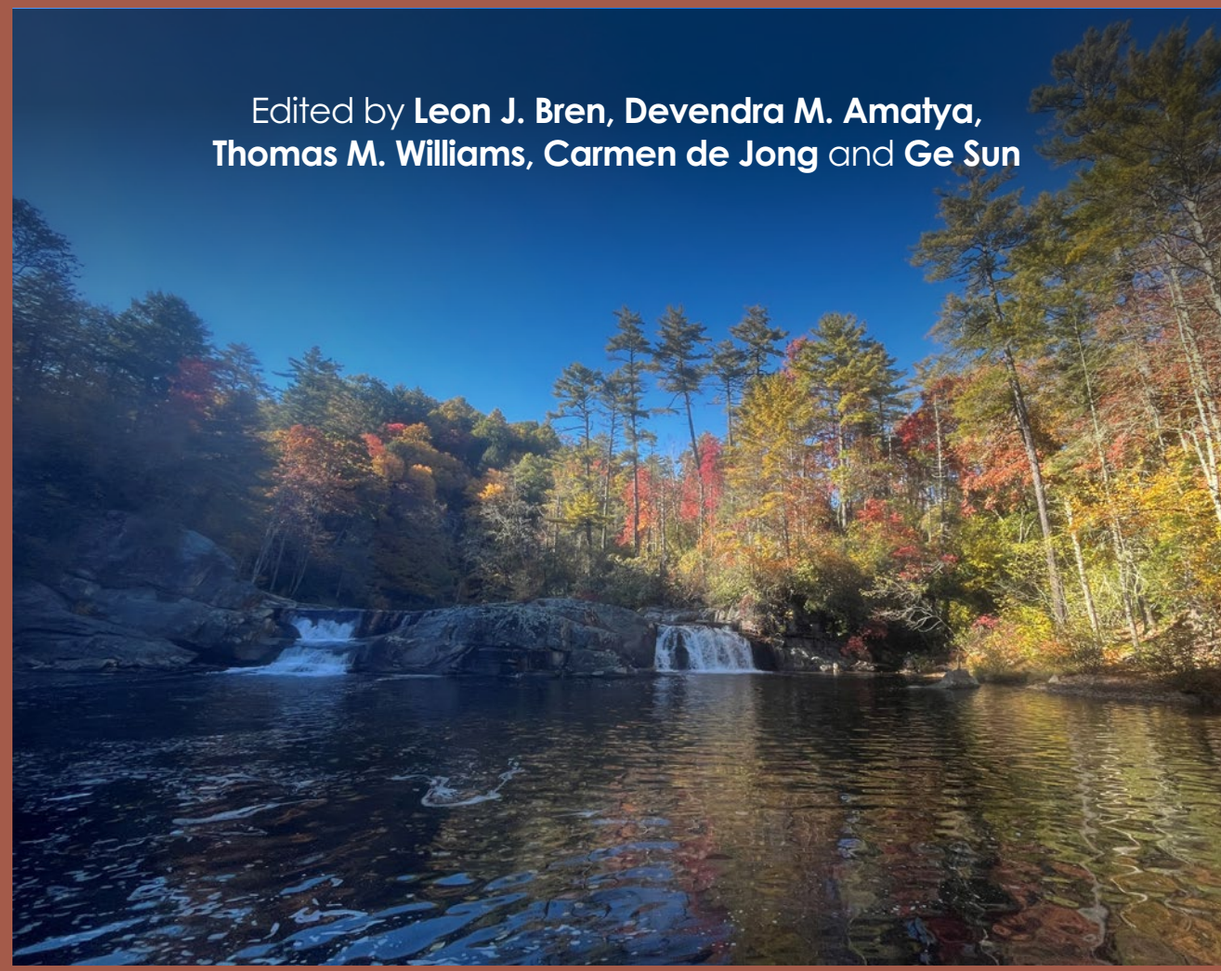

CABI